Journal Name

COMMUNICATION

Perfluoroalkylchain conjugation as a New Tactic for Enhancing Cell Permeability of Peptide Nucleic Acids (PNA) via reducing the Nanoparticle size

Ellipilli Satheesh and Krishna N Ganesh[a,†]

Perfluoro undecanoyl chain conjugated peptide nucleic acids (PNAs) show 2.5 to 3 fold higher cell uptake efficiency in NIH 3T3 and HeLa cells compared to simple undecanoyl PNAs. Fluorination of PNAs leads to formation of lower size (~100-250 nm) nanoparticles compared to larger size (~500 nm) nanoparticles from non-fluorinataed PNAs, thereby improving the effciency of cell penetration.

Nucleic acid therapeutics has emerged as an effective technology for gene inhibition.[1] However, susceptibility towards cellular enzymes and poor cell uptake has limited their applications. In this context chemically modified nucleic acids that resist degradation by the cellular enzymes have attracted greater attention.[2-4] Peptide nucleic acids (PNAs) are a class of DNA mimics derived by replacing the negatively charged sugar phosphate backbone with a pseudo peptide backbone (2-aminoethyl-glycine unit) carrying nucleobases through a tertiary acetamide linker group.[6,7] PNAs bind to complementary DNA and RNA with high affinity, specificity and stable in biological systems.[8,9] The exploration of PNA as antisense agent is limited by their relatively poor cellular uptake[10-12] and has lead to several types of chemical modifications of PNA.[13]

Many methods in the literature that have addressed the issues of efficient cell delivery of PNAs ranging from microinjection,[14] electroporation,[15-17] and co-transfection with DNA using cationic lipids.[18] Although these methods are successful to some extent, they are arduous in protocol and limited to small-scale experimentations. Conjugation of PNAs with cell penetrating peptides[19] and inherently cationic peptides[20] are known to internalize PNAs into cells, with the major fraction localizing in

endosomal compartments, not available for efficient DNA/RNA targeting. Additives like calcium ions and chloroquine are used to release the PNA-peptide conjugates from the endosome, but enhanced potency is often accompanied by pronounced toxicity.[21,22] The self-assembling PNA amphiphiles[23] from PNAs conjugated with di-alkyl lipid tail and charged amino acid residues retained the binding selectivity with DNA,[24] but have not been tested for cell uptake functions. PNA conjugates with cholesterol/cholic acid have been recently shown to be efficient along with a cationic transfection agent in HeLa pLuc705 cells.[25]

The use of cationic polymers or lipids to promote the delivery of antisense ODNs/siRNA[26] though widely reported, have shown considerable cytotoxicity.[27,28] The oligonucleotide conjugates with neutral lipids fare better in enhancing cellular uptake of antisense oligonucleotides/siRNA, prolonging their half-life in plasma and increasing the efficiency of siRNA-induced gene silencing *in vivo*.[29,30-33] Significantly, mere attachment of perfluoroalkyl chains to the 5'-end of the DNA lead to improvement in the cellular localization of the DNA.[34] In this context, we report here the first results of PNAs conjugated with a hydrophobic perfluoro undecanoyl moiety to promote their cell uptake in NIH 3T3 and HeLa cell lines. It is shown that perfluorination of PNAs leads to a decrease in the size of resultant nanoparticles to the 100-250 nm range, more favourable for cell uptake compared 450-500 nm size nanoparticles from non-fluorinated PNAs, an important finding useful for future designs.

Fluorescent PNAs conjugated with undecanoyl and perfluoroundecanoyl moieties were synthesised (Fig. 1) in order to visualize their cellular localization using confocal microscopy. The PNA sequences A (LysNHCO-TGACTCCATT-Lys) and B (LysNHCO-TCACTAGATG-Lys) were synthesized on MBHA solid support using Boc-chemistry by known procedures with standard PNA monomers.[35] N^{α}(tBoc)-N^{ω}(p-Cl-Cbz)-Lysine was first coupled to the MBHA resin, before sequential additions of desired PNA monomers for oligomer synthesis. After the addition of last PNA monomer, N^{α}(Fmoc)-N^{ω}(tBoc)-Lysine was coupled to the PNA at the N-

[a] *Chemical Biology Unit, Indian Institute of Science Education and Research (IISER), Dr Homi Bhabha Road, Pune 411008, Maharashtra, India.*

† JC Bose Fellow, Department of Science and Technology, new Delhi and Honorary Professor, JNCASR, Jakkur, Bengaluru, kn.ganesh@iiserpune.ac.in

terminus, followed by deprotection of ω-amino group by treatment with TFA. This was then coupled with either undecanoic acid or perfluoroundecanoic acid using HBTU/HOBt as coupling reagent under microwave conditions (Figure 1). At the end of synthesis, the resin was treated successively (path A) with piperidine (Fmoc deprotection) and TFA/TFMSA (cleavage from resin) to obtain PNAs 1,2 (sequence A) and PNAs 5,6 (sequence B). In path B, The Fmoc protection on α-amino group of N-terminus lysine was deprotected with piperidine and the free α-amino group was reacted with carboxyfluorescein in the presence of DIC/HOBt as a coupling reagent, followed by cleavage from resin to obtain PNAs **3/4**-CF (PNA sequence A) and PNA **7/8**-CF (sequence B). The non-fluorescent PNAs **1**,**2**,**5** and **6** and the fluorescent PNAs **3, 4, 7,** and **8** were purified by reverse phase C18 HPLC using different gradient elutions. The integrity of synthesised PNAs is supported by their HPLC retention time and mass analysis by MALDI-TOF (Table 1). It is seen that the fluorinated PNAs PNA **2/6** and PNA **4/8-CF** have longer elution times in HPLC than the corresponding non-fluorinated PNAs – PNA **1/5** and PNA **3/7-CF** suggesting a slightly higher hydrophobicity. The identity of fluorinated PNA **2** was also supported by ^{19}F NMR data that gave 5 sets of signals with chemical shifts in the region -122.0 to -127.0 ppm, similar to that seen in the parent perfluoro undecanoic acid (S9, S10 in supporting material).

Table 1 MALDI-TOF spectral analysis of the synthesized PNA oligomers

Entry	PNA	Mol.formula	Calcd m/z	Obsvd m/z	Rt (min)
1	PNA **1**	$C_{130}H_{182}N_{57}O_{35}$	3101.4214[M+H$^+$]	3101.6819	23.6
2	PNA **2**	$C_{130}H_{164}F_{17}N_{57}NaO_{35}$	3429.2432[M+Na$^+$]	3430.3914	27.5
3	PNA **3-CF**	$C_{151}H_{192}N_{57}O_{41}$	3459.4691[M+H$^+$]	3460.2451	13.4
4	PNA **4-CF**	$C_{151}H_{175}F_{17}N_{57}O_{41}$	3765.3090[M+H$^+$]	3765.8383	15.2
5	PNA **5**	$C_{131}H_{182}N_{62}O_{33}$	3151.4469 [M + 2H]	3151.3916	11.9
6	PNA **6**	$C_{131}H_{164}F_{17}N_{62}O_{33}$	3456. 2789 [M + H]	3456.2004	13.1
7	PNA **7-CF**	$C_{152}H_{191}N_{62}O_{39}$	3508.4868 [M + H]	3508.3051	12.9
8	PNA **8-CF**	$C_{152}H_{175}F_{17}N_{62}O_{39}$	3815.3345[M + 2H]	3815.9119	13.9

The cell entry and localization of synthesised PNAs in NIH 3T3 and HeLa cells was explored by confocal imaging to visualize the fluorescent PNAs (PNA **3-CF**, PNA **4-CF,** PNA **7-CF**, and PNA **8-CF**) within the cells. The target cells were incubated for 12 h at standard cell culture conditions (37 $^\circ$C, 5% CO$_2$) in DMEM cell culture medium. The cells were washed with cold PBS and treated with fresh DMEM medium. PNA was added to cells (200 µL) to reach a final concentration of 2 µM and incubated for 24 h after which nuclear stain Hoechst 33442 and ER-tracker (ER-red) were added. After 30 min. the cell medium was aspirated and washed with cold PBS thrice and treated with OPTIMEM cell medium prior to confocal cell imaging. Fig. 2 (NIH 3T3) and Fig 3 (HeLa) show the confocal pictures of cells treated with (A/A') blue Hoechst 33442 (nuclear stain), (B/B') red ER track dye, (C/C') green fluorescent PNA **3**-CF/PNA **4**-CF and (D/D') superimposed pictures of corresponding A, B, C and bright field images. The results suggest that both hydrocarbon (PNA 3-CF) /fluorocarbon (PNA 4-CF) PNAs are taken up by NIH 3T3 and HeLa cells. The green fluorescent PNAs entered into the cytoplasm and co-localized with red ER tracker in the endoplasmic reticulum, leading to yellow colour from the superimposition of green (from PNA) and red (from ER-red tracker) colours. The yellow colour is more intense and focussed in cells treated with fluorinated PNAs (Fig. 2D' and 3D'), compared to the more diffused nature in cells treated with non-fluorinated PNAs in both NIH 3T3 (Fig. 2D) and HeLa (Fig. 3D) cells. This clearly suggests that fluorinated PNAs are more efficient in cell permeation compared to non-fluorinated PNAs and they accumulate in endoplasmic reticulum.

The quantification of the cell uptake by PNA **3**-CF, PNA **4**-CF, PNA **7**-CF, PNA **8**-CF was realised by determining the percent positive cells using fluorescence-assisted cell sorting analysis (FACS) in NIH 3T3 and HeLa cells (Fig. 4). The mean fluorescence was 10 times higher with the fluorinated PNA **4**-CF and PNA **8**-CF than that with non-fluorinated PNA **3**-CF and PNA **7**-CF, although the absolute cell count was slightly lower for fluorinated PNA. However, the percentage of positive cells (Figure 5) with PNA incorporation was 3 fold higher for fluorinated PNA **4**-CF in NIH 3T3 cells and 2 fold more in HeLa cells than with non-fluorinated PNA **3**-CF and PNA **7**-
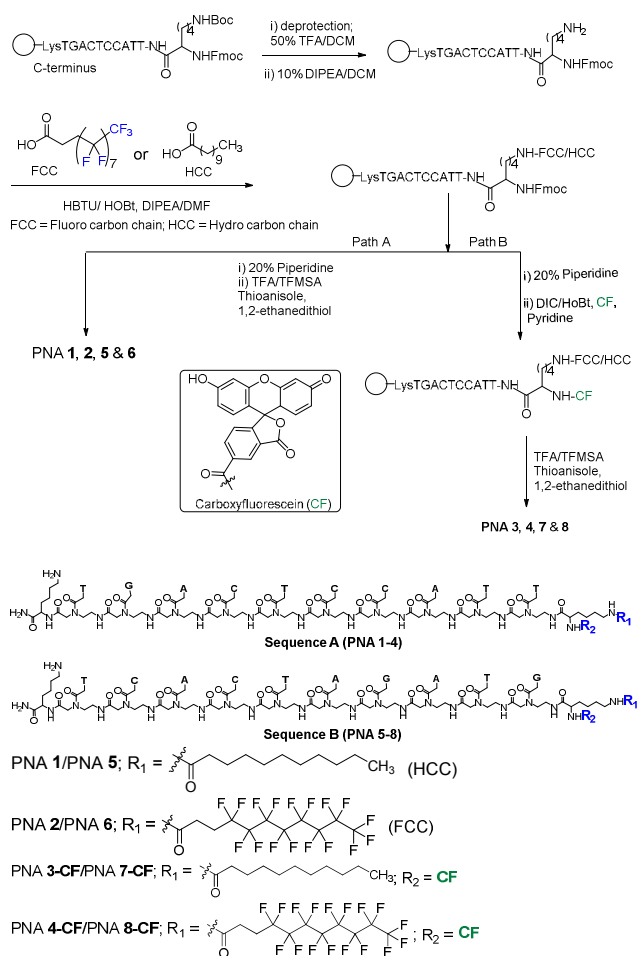

Fig. 1 Solid phase synthesis of alkyl/perfluoroalkyl PNAs.

CF. These data confirm and provide quantitative evidence about the higher competence of fluorinated PNA for cell infiltration.
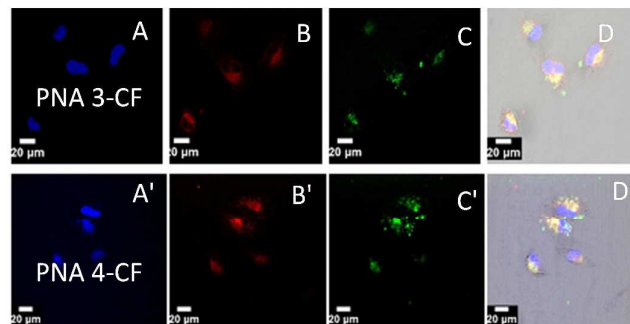

Fig. 2 Confocal images of PNA **3**-CF and PNA **4**-CF in NIH 3T3 cells:(A) Nuclear stain from Hoechst 33442 (B) Red fluorescence image from ER-red, (C) Green fluorescence image from PNA, and (D) Superimposed image of A-c and bright field image.

Fig. 3 Confocal images of PNA **3**-CF and PNA **4**-CF in HeLa cells: (A) Nuclear stain from Hoechst 33442 (B) Red fluorescence image from ER-red, (C) Green fluorescence image from PNA, and (D) Superimposed image of A-C and bright field image.
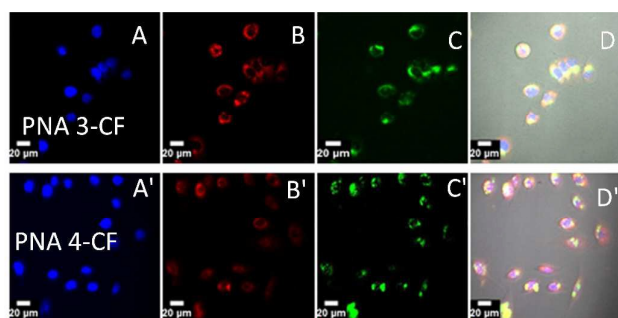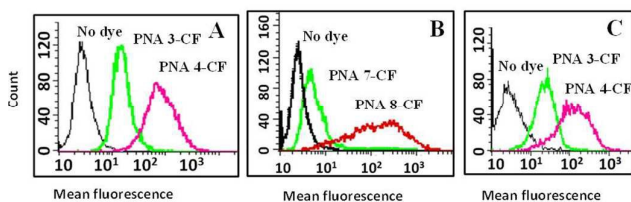

Fig. 4 Overlay histogram of mean fluorescence: (A)&(B) HeLa cells and (C) NIH 3T3 cells; (Black) control cells without dye; (Green) PNA **3**-CF/PNA **7**-CF and (Red) PNA **4**-CF/PNA **8**-CF.

PNAs **1, 2, 5,** and **6** were tested for their self-assembling abilities using FESEM. It was found that these form well-defined nanospheres with particle size in the range ~100-500 nm (Figure 6 and supporting material) compared to the non-fluorinated PNAs-**1** and **5** that formed bigger particles (~450-550 nm). It is important to note that, the perfluoroalkyl chain PNAs (PNA **2** and **6**) produced nanospheres of lesser size of ~100-250 nm. The fluorinated chain
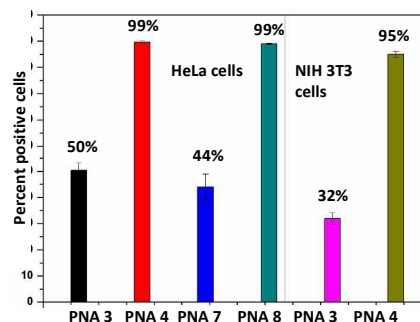

Fig. 5 Percent positive cells in HeLa and NIH 3T3 cells.

in the PNA structure thus seems to cause compaction of the nanoparticle. To examine if this situation exists in solution as well, particle size distribution was measured in aqueous solutions of PNA **1** and PNA **2** by dynamic light scattering technique (S8 in supporting material). It was observed that the particle size distribution in solution was ~~though~~ broader, although the mean size of nanoparticles was around 250 nm for fluorinated PNA **2**, much lower than ~500 nm seen with the non-fluorinated PNA **1**. The nanoparticle size measurements from FESEM correlated well with solution DLS measurements, with fluorinated chain causing 2-fold compaction of nanoparticle size. The particle size of ~100-250 nm is in the right range for effective cell permeation[36] and so perfluoroalkylation of PNA has significant effect on its cell penetrating ability. The results reported here provide a new structure based rationale for engineering future PNAs towards efficient cell delivery.
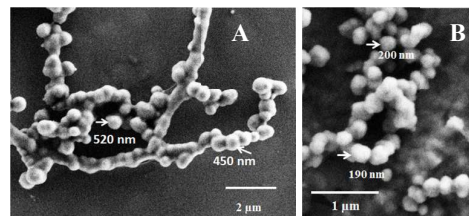

Fig. 6 FESEM images of (A) PNA **1** and (B) PNA **2**.

Perfluoroalkyl/hydrocarbon chain conjugated PNAs can be easily accessed by synthesis on solid support and the protocol is amenable to other chemically modified PNAs as well. The C_{11}-hydrocarbon/ fluorocarbon chain linked at the PNA N-terminus using lysine as a linker also enabled attachment of fluorophore as well. Both NIH3T3 and HeLa cells take up fluorocarbon/hydrocarbon conjugated PNAs and localise them in endoplasmic reticulum as followed by red ER-tracker dye and seen as intense yellow colour in superimposed images in confocal microscopy. The perfluorocarbon PNA was taken up in higher quantity (Fig. 4, mean fluorescence) and by more ~~number~~ of the cells (Fig. 5) than the non-fluorinated PNA. Significantly, the conjugated perfluorocarbon chain on PNA induces formation of nanoparticle of ~200 nm size that may promote their higher efficiency of uptake by cells than the higher (~500 nm) particle size of non-fluorinated PNA. Thus perfluroalkylation is a

convenient and useful addition to a growing repertoire of rational strategies to overcome the poor cell permeability of PNAs. We have recently shown that introduction of difluoromethylene units in the *apg*-PNA backbone has similar cell permeation enhancing effect, but much lower than the perfluoroalkylation reported here.[37] It has good potential to be an "add-on" device in combination with other chemical modifications such as cationic guanidinalation[20] to generate hybrid peptide nucleic acids to access intracellular targets either as an aptamer[38] or as a gene silencing agent. The interesting self-assembling properties induced by perfluorocarbon chains may also be explored towards new applications of PNA in material science.[39]

Notes and references

1. C. A. Stein, *Pharmacol. Ther.,* 2000, **85**, 231.
2   J. B. Opalinska and A. M. Gewirtz, *Nature Rev. Drug Discov.,* 2002, **1**, 503.
3.   C. F. Bennett and E. E. Swayze, *Ann. Rev. Pharm. Toxicol.,* 2009, **50**, 259.
4. R. Kole, A. R. Krainer and S. Altman*, Nature Rev. Drug Discov.,* 2012, **11**, 12*5*
5. S. L. DeVos and T. M. Miller, *Neurotherapeutics*. 2013, **10**, 486.
6. P. E. Nielsen, M. Egholm, R.H. Berg and O. Buchardt, *Science,* 1991, **254**, 1497.
7. M. Egholm, O. Buchardt, P. E. Nielsen and R. H. Berg, *J. Am. Chem. Soc.,* 1992, **114**, 1895.
8. H. Kuhn, V. V. Demidov, P. E. Nielsen and M. D. Frank-Kamenetskii, *J. Mol. Biol.,* 1999, **286**, 1337.
9. V. V. Demidov, V. Potaman, M. D. Frank-Kamenetskii, M. Egholm, O. Buchard, S. H. Sonnichsen and P. E. Nielsen, *Biochemical Pharmacology,* 1994, **48**, 1310.
10. U. Koppelhus, P. E. Nielsen, *Adv. Drug Del. Rev.* 2003, **55**, 267.
11. M. A. Bonham, S. Brown, A. L. Boyd, P. H. Brown, D.A. Bruckenstein, J. C. Hanvey, S. A. Thomson, A. Pipe, F. Hassman, J. E. Bisi, B. C. Froehler, M. D. Matteucci, R. W. Wagner, S. A. Noble and L. E. Babiss, *Nucleic Acids Res.,* 1995, **23**, 1197.
12. P. Wittung, J. Kajanus, K. Edwards, P. E. Nielsen, B. Norden and B. G. Malmström, *FEBS Letters.,* 1995, **365**, 27.
13. (a) V.A. Kumar, K.N. Ganesh, *Acc. Chem. Res.* 2005, **38**, 404. (b) Sugiyama T and Kittaka A, *Molecules* 2013, **18**, 287.
14. J. C. Hanvey, N. J. Peffer, J. E. Bisi, S. A. Thomson, R. Cadilla, J. A. Josey, D. J. Ricca, C. F. Hassman, M. A. Bonham, K. G. Au, *et al. Science,* 1992, **258**, 1481.
15. M. A. Shammas, C. G. Simmons, D. R. Corey and R. J. Shmookler Reis, *Oncogene,* 1999, **18**, 6191.
16. J. G. Karras, M. A. Maier, T. Lu and A. Watt, M. Manoharan, *Biochemistry,* 2001, **40**, 7853.
17. G. Wang, X. Xu, B. Pace, D. A. Dean, P. M. Glazer, P. Chan, S. R. Goodman and I. Shokolenko, *Nucleic Acids Res.,* 1999,**27**, 2806.
18. B. Herbert, A. E. Pitts, S. I. Baker, S. E. Hamilton, W. E. Wright, J. W. Shay and D. R. Corey, *Proc. Natl. Acad. Sci. U S A.,* 1999, **96**, 14276.
19. P. E. Nielsen, *Q. Rev. Biophys*., 2005, **38**, 345.
20. (a) D. R. Jain, L. V. Anandi, M. Lahiri, K. N. Ganesh, *J. Org. Chem.* 2014, **79**, 9567. (b) B. Sahu, V. Chenna, K.L. Lathrop, S.M.

Thomas, G. Zon, K. J. Livak, D. H. Ly, *J. Org. Chem.*, 2009, **74**, 1509.
21. T. Shiraishi, S. Pankratova and P. E. Nielsen, *Chem. Biol.*, 2005, **12**, 923.
22. J. Hu and D. R. Corey, *Biochemistry,* 2007, **46**, 7581.
23. J. P. Vernille, L. C. Kovell and J. W. Schneider, *Bioconjugate Chem.,* 2004,**15**,1314.
24. B. F Marques and J. W. Schneider, *Langmuir,* 2005, **21**, 2488.
25. T. Shiraishi and P. E. Nielsen, *Bioconjugate Chem.,* 2012, **23**, 196.
26. T. Geisbert, W. A. C. Lee, M. Robbins, J. B. Geisbert, A. N. Honko, V. Sood, J. C. Johnson, S. de Jong, I. Tavakoli, A. Judge, L. E. Hensley and I. Maclachlan, *Lancet,* 2010**, 375**, 1896.
27. N. Al-Brahim and S. L. Asa, *Arch. Pathol. Lab. Med.,* 2006, **130**, 1057.
28. W. T. Kuo, H. Y. Huang and Y. Y. Huang, *Curr. Drug. Metab*., 2009, **10**, 885.
29. J. Soutschek, A. Akinc, B. Bramlage, K. Charisse, R. Constien, M. Donoghue, S. Elbashir, A. Geick, P. Hadwiger, J. Harborth, M. John, V. Kesavan, G. Lavine, R. K. Pandey, T. Racie, K. G. Rajeev, I. Rohl, I. Toudjarska, G. Wang, S. Wuschko, D. Bumcrot, V. Koteliansky, S. Limmer, M. Manoharan and H. P. Vornlocher, *Nature,* 2004**, 432**, 173.
30. C. Wolfrum, S. Shi, K. N. Jayaprakash, M. Jayaraman, G. Wang, R. K. Pandey, K. G. Rajeev, T. Nakayama, K. Charrise, E. M. Ndungo, T. Zimmermann, V. Koteliansky, M. Manoharan and M. Stoffel, *Nat. Biotechnol.,* 2007, **25**, 1149.
31. Y. Ueno, K. Kawada, T. Naito, A. Shibata, K. Yoshikawa, H. S. Kim, Y. Wataya and Y. Kitade, *Bioorg. Med. Chem*., 2008**, 16**, 7698.
32. P. C. de Smidt, T. Le Doan, S. de Falco and T. J. van Berkel, *Nucleic Acids Res*., 1991, **19**, 4695.
33. M. Raouane, D. Desmaële, G. Urbinati, L. Massaad-Massade and P. Couvreur, *Bioconjugate Chem.,* 2012, **23**, 1091.
34. G. Godeau, H. Arnion, C. Brun, C. Staedel and P. Barthelemy, *MedChemComm,* 2010, **1**, 76.
35. Koch, T. PNA Synthesis by Boc Chemistry. In Peptide Nucleic Acids: Protocols and Applications; 2nd ed.; P. E. Nielsen, Eds.; Horizon Scientific Press: Norfolk, U.K., 2004; pp 37.
36. (a) J. Y. Yhee, S. Lee and K. Kim, *Nanoscale*, 2014, **6**, 13383. (b) Y. H. Bae, K. Park, *Journal of Controlled Release* 2011, **153**, 198.
37. S. Elipilli, K. N. Ganesh, *J. Org. Chem*.,2015, **80**, 9185.
38. E. J. Lee, H. K. Lim, Y. S. Cho and S. S. Hah, *RSC Advances*, 2013, **3**, 5828.
39. L-H. Liu, Z-Y. Li, L. Rong, S-Y. Qin, Q. Lei, H. Cheng, X. Zhou, R-X. Zhuo and X-Z. Zhang, *ACS Macro Lett.,* 2014, **3**, 467.